STABILIZATION OF SATELLITE MOTION RELATIVE TO A COULOMB SPACECRAFT FORMATION

Hanspeter Schaub

Simulated Reprint from

Journal of Guidance, Navigation and Control

Volume 28, Number 6, July–Aug., 2006, Pages 831–839

A publication of the
American Institute of Aeronautics and Astronautics, Inc.
1801 Alexander Bell Drive, Suite 500
Reston, VA 22091

JOURNAL OF GUIDANCE, NAVIGATION AND CONTROL
Vol. 28, No. 6, July–Aug., 2006

STABILIZATION OF SATELLITE MOTION RELATIVE TO A COULOMB SPACECRAFT FORMATION

Hanspeter Schaub*

Coulomb spacecraft are satellites which can actively control their electrostatic charge, and thus exploit inter-vehicle electrostatic forces to control tight relative motion. The stabilization problem of a cluster of unequal Coulomb spacecraft is studied. Previous research has developed a nonlinear control law to stabilize the relative motion of one satellite relative to another. With only two spacecraft present, with equal mass and charging limits, Newton's second law greatly simplified the control development. This control strategy is generalized here to stabilize the relative motion of a satellite relative to a larger cluster of Coulomb spacecraft with unequal satellite masses and individual charge saturation limits. The chief cluster motion can be either circular or elliptic. The nonlinear control methodology exploits an orbit element difference description of the satellite relative motion. While the control is shown to stabilize the relative motion of a Coulomb satellite about any set of desired orbit element differences, convergence is shown thus far only when controlling exclusively the semi-major axis differences. Thus, this control is able to achieve bounded relative motion of the Coulomb satellite, even in the presence of saturation constraints. A simple structured control approach is numerically investigated to control the entire cluster. Numerical simulations illustrate the relative motion control behavior with the cluster chief or center of mass being on an elliptic high Earth orbit.

Introduction

A geosynchronous (GEO) satellite is exposed to a space plasma environment that contains positively charged ions and negatively charged electrons. The faster electrons will accumulate more rapidly on the craft than the slower positively charged ions. This causes a negative electric charge build-up to occur within the spacecraft. At steady-state charging conditions, the negative electric field about the spacecraft will repel a sufficiently large number of electrons such that a zero net current to the craft will result. Depending on the space plasma density, the steady-state charges can vary from near-zero to several kilovolts. In 1979 the SCATHA satellite[1] was launched. One of its goals was to measure the build-up and breakdown of electrostatic charge on various spacecraft components, as well as to actively control the spacecraft charge using an electron beam. This mission was able to flight verify that it is possible to actively control the spacecraft charge. If another spacecraft had been present with a separation distance of about 20 meters, the natural uncontrolled SCATHA voltage levels would have been enough to impose inter-spacecraft forces in the milli-Newton level.[2] The amount of electrical power required to generate these active electrical fields is less than 1 Watt. An ion engine operates by expelling charged particles (ions) at a very high velocity. The force generated is due to the momentum exchange between the particle and the spacecraft. To control the spacecraft charge, a comparable device to an ion engine would be used. Here the ion exit velocity would have to be large enough for the particle to escape the local electrical potential field. To achieve a certain thrust level, a traditional ion engine will expel a larger amount of ions, to produce the needed change in momentum, than a Coulomb ion engine, which only has to expel enough ions to generate a specific electric field.[2] This leads to the Coulomb force production having a drastically lower electrical power requirement than ion thrust production. The force exerted onto the Coulomb spacecraft due to momentum exchange with the expelled particle is negligible. The Coulomb satellite will only experience a force if additional *charged* spacecraft are in the vicinity. Similarly, the amount of mass expelled (charged ion particles) is so small that this mode of navigation control is referred to as being "essentially propellantless."[3] A recent example of active spacecraft electric potential control using an ion source is found in Reference 4. Here the first results of the CLUSTER mission are discussed where the spacecraft charge is held near zero in a low-density space plasma environment.

Note that such Coulomb forces will *only* control the relative motion of the satellite cluster, not the inertial motion of the cluster center of mass. For example, it would be impossible to use such Coulomb forces to boost the spacecraft cluster overall orbit altitude. However, it is possible to control the relative motion between the Coulomb satellites by changing the satellite charges. Thus, the Coulomb Formation Flying (CFF) concept allows for very fuel-efficient relative navigation with a very high control bandwidth. For example, in Reference 2 a 1 meter spacecraft was found to be able to charge to 6 kV in as little as 8 ms using only 200 mW of power. The CFF concept could be used for general proximity flying (fly a sensor about a larger craft) or for controlling the relative motion of swarms or clusters of satellites. Since the magnitude of the Coulomb electrostatic force diminishes with $1/r^2$ of the separation distance, it is only effective for relatively tight formation/proximity flying scenarios of 10-100 meters. For minimum separation distances larger than that, the required spacecraft charging levels simply become impractical. Further, the Coulomb force effectiveness is diminished in a high density space plasma environment. This is typically measured through the Debye length λ_d which indicates the exponential decay e^{-r/λ_d} of the electrostatic field strength in a plasma environment.[5,6] This decay is in addition to the natural point charge $1/r^2$ field strength reduction. For example, at LEO the Debye length is on the order of centimeters, thus preventing electrostatic forces from being an effective relative motion control method. At GEO, in comparison, the Debye length is of the order of 100 and 1000 meters, depending on the current plasma density conditions. Formation flying missions with such small relative orbits are useful to perform high accuracy, very wide field of view missions, or to measure local gradients in the space environment.

Developing control laws for such CFF concepts are challenging in that the charge dynamics are highly nonlinear and coupled. By changing the charge of a single satellite, the net resulting electrostatic force experienced by all other charged craft in the cluster will be changed as well. In Reference 3, 7 static equilibrium solutions are presented of the CFF concept where the formation center of mass is assumed to be in a circular orbit. Interesting in-plane two dimensional solutions, as well general three-dimensional solutions are found. However, none of the equilibrium solutions found so far are stable and would require an active charge control law to be developed. A control solution for a simplified two-spacecraft formation with equal satellite mass is presented in Reference 7. The control law is based on an orbit element difference description of the relative motion and applies to both circular and elliptical cluster center of mass motion. While this control was shown to globally stabilize the motion of one satellite relative to a single additional satellite, it was not asymptotically stabilizing for all initial conditions. For example, if the initial formation has only in-plane satellite motion, and the final formation is to have out-of-plane motion, then such a relative orbit correction cannot be achieved with only inter-satellite forces. However, for the case of controlling only the semi-major axis differences δa of the satellites, it was shown that the control was indeed asymptotically stabilizing. As a result, the two-spacecraft control law was able to balance the semi-major axis of both satellites and achieve bounded relative motion.

This paper explores controlling the relative motion of a Coulomb Spacecraft Formation (CSF) containing more than two satellites. The satellites are also no longer assumed to have equal masses, and may also have individual charging limits. An orbit element differ-

*Assistant Professor, Aerospace and Ocean Engineering Department, Virginia Polytechnic Institute, Senior AIAA Member.

Presented as Paper 04-259 at the 14th AAS/AIAA Space Flight Mechanics Meeting, Maui, Hawaii, Feb. 8–12, 2004.

ence approach is used to describe the relative motion and relative motion errors. A centralized nonlinear control strategy is investigated where the relative motion error of a single satellite versus the formation chief is corrected one at a time. The stability and convergence of the single craft control is discussed. A simple structured control approach is investigated to stabilize the relative motion of the entire cluster. The resulting control is applicable to controlling both circular and elliptical cluster center of mass orbits. Numerical simulations are shown to illustrate the control performance and behavior.

CSF Equations of Motion

Consider a formation or cluster of N Coulomb satellites each with mass m_i. The inertial equations of motion of the i-th spacecraft are given by

$$\ddot{\boldsymbol{r}}_i = -\frac{\mu}{r_i^3}\boldsymbol{r}_i + \boldsymbol{\alpha}_i + \boldsymbol{a}_i \tag{1}$$

where $\boldsymbol{r}_i$ is the inertial position vector, $r = |\boldsymbol{r}_i|$ is the current inertial orbit radius, $\boldsymbol{\alpha}_i$ is the acceleration due the the electrical charges of the other spacecraft, and $\boldsymbol{a}_i$ is the non-Keplerian acceleration (for example, due to J_2 or atmospheric drag). For the purpose of the control analysis, the acceleration vector $\boldsymbol{a}_i$ is set to zero. However, when running numerical simulations, the J_2–J_5 gravitational accelerations are included. Let $\boldsymbol{E}_i$ be the electrostatic field vector experienced by the i-th spacecraft. If the craft has a charge q_i, then the electrostatic force $\boldsymbol{F}_i$ applied to the craft is

$$\boldsymbol{F}_i = q_i \boldsymbol{E}_i \tag{2}$$

and the corresponding acceleration $\boldsymbol{\alpha}_i$ is expressed as

$$\boldsymbol{\alpha}_i = \frac{1}{m_i}\boldsymbol{F}_i \tag{3}$$

If N satellites are present in a CSF, then the electric field $\boldsymbol{E}_i$ that satellite i will experience due to the other satellites is given by

$$\boldsymbol{E}_i = k_c \sum_{j=1}^{N} q_j \frac{\boldsymbol{r}_{ji}}{|\boldsymbol{r}_{ji}|^3} e^{-\frac{|\boldsymbol{r}_{ji}|}{\lambda_d}} \qquad \text{for } i \neq j \tag{4}$$

where $\boldsymbol{r}_{ji} = \boldsymbol{r}_i - \boldsymbol{r}_j$ is the relative position vector, and $k_c = 8.99 \cdot 10^9 \mathrm{Nm}^2/\mathrm{C}^2$ is Coulomb's constant. Note that we have not assigned any coordinate frame to this potential field expression. As such, the given expression is valid for both an inertial and Hill frame specific equations of motion description. The parameter λ_d is the Debye length. For analysis purposes, this parameter is assumed to be infinitely large and the exponential term in Eq. (4) is thus ignored. During numerical simulations, it is set to a finite value to illustrate robustness of the control to this effect.

Besides using inertial Cartesian coordinate position vectors $\boldsymbol{r}$, the spacecraft motion can also be described through orbit elements. Let $\boldsymbol{\sigma e}_i$ be a six dimensional orbit element vector of the i-th spacecraft. These elements are invariants of the non-perturbed motion, just as the initial conditions $\boldsymbol{r}(t_0)$ and $\dot{\boldsymbol{r}}(t_0)$ are invariants of the Cartesian motion description. From Gauss' variational equations,[8,9] given an external acceleration vector $\boldsymbol{u}_i$, the orbit element vector $\boldsymbol{\sigma e}_i(t)$ will evolve according to

$$\dot{\boldsymbol{\sigma e}}_i = [\mathcal{B}(\boldsymbol{\sigma e}_i, f_i)]\boldsymbol{u}_i \tag{5}$$

where $[\mathcal{B}(\boldsymbol{\sigma e}_i, f_i)]$ is a 6×3 control influence matrix. This matrix depends on both the current satellite orbit element set $\boldsymbol{\sigma e}_i$ and the associated time-dependent true anomaly angle f_i. Note that no specific choice of orbit elements is being performed at this point in the development. The spacecraft charge control law presented is independent of the type of chosen orbit elements. The control development will utilize the equations of motion shown in Eq. (5), while numerical illustrations will use the equations of motion shown in Eq. (1).

Control Law Strategy

Assume that the desired relative motion is expressed through the fixed orbit element difference vector $\Delta\boldsymbol{\sigma e}_i$ relative to the formation chief or center of mass motion. The formation internal electrostatic forces will have an influence on the center of mass motion. This is comparable to the classical attitude and orbital motion coupling of a rigid body in space. However, the center of mass motion departure from Keplerian orbital motion is very small given the very small relative orbit dimension of 10-100 meters, and is thus neglected here. Thus, the chief or formation center of mass orbit elements $\boldsymbol{\sigma e}_c$ will be a constant vector in this development. In References 9–12 the control law

$$\boldsymbol{u}_i = -[\mathcal{B}(\boldsymbol{\sigma e}_c, f_c)]^T [K] \delta\boldsymbol{\sigma e}_i \tag{6}$$

has been shown to be asymptotically stabilizing for Keplerian satellite motion if arbitrary control accelerations $\boldsymbol{u}_i$ can be implemented through the propulsion system. Here the gain matrix $[K]$ must be a 6×6 symmetric, positive definite matrix, while $[\mathcal{B}(\boldsymbol{\sigma e}_c, f_c)]$ is the chief orbit 6×3 control influence matrix of Gauss' variational equation.[8,9] While $\boldsymbol{\sigma e}_c$ is assumed to be a constant vector, the chief true anomaly angle f_c is time dependent. Note that this control law is applicable to both circular and elliptic chief orbits. Further, the tracking errors can be expressed using differences of various types of orbit elements such as the classical orbit element set, or equinoctial orbit elements.[13]

In Reference 7 a nonlinear control strategy is developed for a CSF of two equal satellites which exploits the control law in Eq. (6). Because two spacecraft can only exert an electrostatic force onto each other along their relative position vector $\boldsymbol{r}_{ij}$, we cannot generate arbitrary control accelerations $\boldsymbol{u}_i$. Instead, the control solution $\boldsymbol{u}_i$ is projected along the relative position vector direction of the two satellite system to develop a stabilizing charging control law $q_i(t)$ for each craft. The control development and stability analysis used a vector dot product to perform the projection and is only applicable to a two-satellite formation of equal mass. The following development will generalize and expand this control idea to attempt to control a satellite relative to a larger formation of Coulomb satellites.

Unsaturated Control

Let $\boldsymbol{\epsilon}_i$ be a vector of dimension $M \leq 6$ containing the orbit elements which are to be controlled. This formulation allows us to control as few as a single orbit element difference, or several orbit element differences up to a total of six. Assume that the desired relative orbit motion is prescribed through a constant orbit element difference vector $\Delta\boldsymbol{\epsilon}_i$. The tracking error dynamics are given by

$$\delta\dot{\boldsymbol{\epsilon}}_i = \dot{\boldsymbol{\epsilon}}_i - \dot{\boldsymbol{\epsilon}}_c - \Delta\dot{\boldsymbol{\epsilon}} = \dot{\boldsymbol{\epsilon}}_i = [B(\boldsymbol{\sigma e}_i, f_i)]\boldsymbol{\alpha}_i \tag{7}$$

where $\boldsymbol{\alpha}_i$ is the actual control acceleration vector being applied to the i-th spacecraft (with vector components taken in the local LVLH frame), and the $M \times 3$ matrix $[B(\boldsymbol{\sigma e}_i, f_i)]$ is the control influence matrix of $\boldsymbol{\epsilon}$. Note that the tracking error is written here relative to the formation center of mass, while with the two-satellite formations in Reference 7 the tracking error was written as the error of one satellite relative to the other. Further, note that $[B(\boldsymbol{\sigma e}_i, f_i)]$ is a subset of the full $[\mathcal{B}(\boldsymbol{\sigma e}_i, f_i)]$ matrix from Gauss' variational equations in Eq. (5). Let the orbit element difference vector $\delta\boldsymbol{\sigma e}_i = \boldsymbol{\sigma e}_i - \boldsymbol{\sigma e}_c$ describe the actual spacecraft relative motion with respect to the formation barycenter, and $\delta f_i = f_i - f_c$ be the associated true anomaly difference. Because the relative orbits radii considered in CSFs are very small, of the order of 10's to 100's of meters, and $\delta\boldsymbol{\sigma e}_i \ll \boldsymbol{\sigma e}_c$ and $\delta f_i \ll f_c$, the $[B]$ matrix is modeled through the approximation:[9–12]

$$\begin{aligned}[B(\boldsymbol{\sigma e}_i(t), f_i(t))] &= [B(\boldsymbol{\sigma e}_c + \delta\boldsymbol{\sigma e}_i(t), f_c + \delta f_i(t))] \\ &\approx [B(\boldsymbol{\sigma e}_c, f_c(t))] = [B(t)]\end{aligned} \tag{8}$$

The tracking error dynamics are then written as

$$\delta\dot{\boldsymbol{\epsilon}}_i = [B(t)]\boldsymbol{\alpha}_i \tag{9}$$

Note that the explicit dependencies of the $[B]$ matrix have been dropped here for notational convenience and readability. This matrix $[B(t)]$, as well as the shown tracking error dynamics, are time dependent because f_c is time dependent. Thus the dynamical system is non-autonomous.

Let us assume that we are only going to control the tracking error of a single satellite. Without loss of generality, assume that the N-th satellite has the worst tracking error $\delta\boldsymbol{\epsilon}_i$. The acceleration $\boldsymbol{\alpha}_N$ experienced by this N-th satellite due the the Coulomb charge of the other $L = N - 1$ satellites is

$$\boldsymbol{\alpha}_N = \frac{q_N}{m_N} k_c \left(q_1 \frac{\hat{\boldsymbol{r}}_{1N}}{r_{1N}^2} + \cdots + q_L \frac{\hat{\boldsymbol{r}}_{LN}}{r_{LN}^2} \right) \tag{10}$$

where $\hat{\boldsymbol{r}}_{ij} = \boldsymbol{r}_{ij}/r_{ij}$ is a unit relative position vector. Let the L-dimensional vector $\boldsymbol{Q}$ be defined as a vector of charge products through

$$\boldsymbol{Q} = \begin{pmatrix} Q_{1N} \\ \vdots \\ Q_{LN} \end{pmatrix} = \begin{pmatrix} q_1 q_N \\ \vdots \\ q_L q_N \end{pmatrix} \tag{11}$$

while the $3 \times L$ dimensioned, time-dependent matrix $[A(t)]$ is defined as

$$[A(t)] = \begin{bmatrix} \frac{\hat{\boldsymbol{r}}_{1N}(t)}{r_{1N}^2(t)} & \cdots & \frac{\hat{\boldsymbol{r}}_{LN}(t)}{r_{LN}^2(t)} \end{bmatrix} \tag{12}$$

The acceleration vector $\boldsymbol{\alpha}_N$ can now be written as

$$\boldsymbol{\alpha}_N = \frac{k_c}{m_N} [A(t)] \boldsymbol{Q} \tag{13}$$

Next the actual acceleration is set equal to a stabilizing control acceleration $\boldsymbol{u}_N$.

$$\boldsymbol{\alpha}_N = \frac{k_c}{m_N} [A(t)] \boldsymbol{Q} = \boldsymbol{u}_N \tag{14}$$

Note that this control acceleration is the control law shown in Eq. (6), but it could be any stabilizing control law. If the matrix $[A]$ has a rank less than 3, then the condition $\boldsymbol{\alpha}_N = \boldsymbol{u}_N$ cannot be achieved exactly. Instead, an approximate least squares solution will be used. If the $L \times 3$ matrix $[A]$ is full rank, then there are an infinity of charge solutions that will satisfy $\boldsymbol{\alpha}_N = \boldsymbol{u}_N$. In this case, a minimum-norm inverse solution will be used. Using the pseudo-inverse of the matrix $[A]$, we can solve Eq. (14) for the charge product vector $\boldsymbol{Q}$ for all rank cases of $[A]$ as

$$\boldsymbol{Q} = \frac{m_N}{k_c} [A(t)]^\dagger \boldsymbol{u}_N \tag{15}$$

where $L \times 3$ dimensioned matrix $[A]^\dagger$ is the pseudo-inverse of the matrix $[A]$. If $L = 1$, as is the case with the two-satellite formation in Reference 7, then $[A]^\dagger = r_{1N}^2 \hat{\boldsymbol{r}}_{1N}^T$ and the control law of Reference 7 is regained. Please note that while the ideal stabilizing control law $\boldsymbol{u}_N = \boldsymbol{u}_N(\delta\boldsymbol{\epsilon}_N)$ depends only on orbit element differences, the charging control law for $\boldsymbol{Q}$ in Eq. (15) depends both on orbit element tracking errors $\delta\boldsymbol{\epsilon}_i$ and the Cartesian relative position vectors $\boldsymbol{r}_{iN}$ through the $[A]$ definition in Eq. (12). Thus, the charge control solution is a hybrid Cartesian and orbit element difference based formulation.

Note that the charging control law in Eq. (15) only defines what the charge products $q_i q_N$ should be, not what the individual charges actually are. There are many methods to extract the individual charges. The following method was adopted in this paper. After computing the $\boldsymbol{Q}$ vector, the Q_{iN} term is found which has the largest magnitude $Q_{\max}$. The charge of the N-th spacecraft is then set to

$$q_N = \sqrt{Q_{\max}} \tag{16}$$

The other L charges are then computed using

$$q_i = \frac{Q_{iN}}{q_N} \qquad \text{for } i = 1, \cdots, L \tag{17}$$

Note that with this charging law, the q_N charge is always positive, while the other charges can be either positive or negative, depending on the sign of the Q_{iN} term.

Substituting the pseudo-inverse charging law in Eq. (15) into the acceleration vector computation in Eq. (14), we find the actual spacecraft acceleration vector to be

$$\boldsymbol{\alpha}_N = \frac{k_c}{m_N} [A] \frac{m_N}{k_c} [A]^\dagger \boldsymbol{u}_N = [A][A]^\dagger \boldsymbol{u}_N \tag{18}$$

Only if the rank of $[A]$ is 3, then $[A][A]^\dagger = [I_{3\times 3}]$ and the condition $\boldsymbol{\alpha}_N = \boldsymbol{u}_N$ is satisfied. If the rank of $[A]$ is 3 and $L > 3$, then this $\boldsymbol{Q}$ computation provides a minimum norm solution. If the rank of $[A]$ is less than 3, then this $\boldsymbol{Q}$ computation provides a least-squares solution. Where for the two-satellite control solution in Reference 7 the charging always corresponded to a least-squares solution, the use of the pseudo-inverse here allows this control strategy to be scaled to all available matrix rankings and dimensions.

The typical spacecraft charge values can be as large as 10's of μC. However, when computing the Q_{ij} terms, note that numerical issues may arise if the average spacecraft charge falls below 0.01 μC. In this case the product of the charges is 10^{-16} C or less, which causes problems with the typical 16 digits of computer accuracy. To avoid this issue when numerically computing the charging product vector Q in Eq. (15), the charges are non-dimensionalized by the individual maximum allowable spacecraft charges. In non-dimensional charge units, a value of 1 for a craft means that the maximum craft charging limit has been reached. When computing the actual charges using Eq. (17), the non-dimensional charge product value Q_{iN} would have to be dimensionalized first.

This control will only stabilize the motion of a single satellite relative to the remaining CSF. To attempt to stabilize the relative motion of the entire cluster, a simple structured control strategy is investigated. During the first step, we find the satellite with the worst tracking error $\delta\boldsymbol{\epsilon}$ and give it the label N. Next the remaining L satellites electric charges q_i are exploited to reduce this tracking error. While controlling the N-th satellite, the tracking errors of the other satellites is monitored. If another satellite is found to have the worst tracking error of the formation, then the structured control will relabel this satellite to be the N-th satellite, and use the remaining formation to reduce it's tracking error. The mathematical formulation is general enough such that the cluster can consist of $N \geq 2$ satellites. Alternatively, another switching logic approach would drive the tracking errors of one satellite to nearly zero, and only then switch to control another satellite. However, please note that no performance or stability claims are made while the switching occurs. Only the tracking errors of the Nth satellite are guaranteed to be stable while the remaining formation is used to control the Nth satellite position. Numerical examples will illustrate that this simple switching strategy does appear to stabilize the semi-major axis tracking errors of a three satellite formation, not just a single satellite. However, for larger formation, a more sophisticated switching structure will be required.

Un-Saturated Control Stability Analysis

Assuming that the craft can achieve unlimited amounts of charge q_i, we would like to study the stability of the charging control law outlined in Eqs. (15)–(17). To do so, we define the Lyapunov function V in terms of the relative orbit tracking error $\delta\boldsymbol{\epsilon}$.

$$V(\delta\boldsymbol{\epsilon}) = \frac{1}{2} \delta\boldsymbol{\epsilon}^T [K] \delta\boldsymbol{\epsilon} \tag{19}$$

where $[K]$ is a $M \times M$ symmetric, positive definite gain matrix. The charging control law $\boldsymbol{Q}$ in Eq. (15) is stabilizing for the non-autonomous dynamical system $\delta\dot{\boldsymbol{\epsilon}} = \delta\dot{\boldsymbol{\epsilon}}(\delta\boldsymbol{\epsilon}, t)$ if it can be shown that the function V is positive definite, decrescent, and $\dot{V} \leq 0$.[14,15] Because the chosen $V(\delta\boldsymbol{\epsilon})$ function does not depend explicitly on time, by inspection it is found to be both positive definite and decrescent. Taking the derivative of $V(\delta\boldsymbol{\epsilon})$ and using the tracking error dynamics $\delta\dot{\boldsymbol{\epsilon}}_N = [B(t)]\boldsymbol{\alpha}_N$ in Eq. (7) leads to

$$\dot{V} = \delta\boldsymbol{\epsilon}^T [K] \delta\dot{\boldsymbol{\epsilon}} = \delta\boldsymbol{\epsilon}^T [K][B(t)] \boldsymbol{\alpha}_N \tag{20}$$

Using the spacecraft acceleration expression in Eq. (18) and the ideal control expression in Eq. (6), $\dot{V}$ is written as

$$\begin{aligned}\dot{V} &= -\delta\boldsymbol{\epsilon}^T[K][B(t)][A(t)][A(t)]^\dagger[B(t)]^T[K]\delta\boldsymbol{\epsilon} \\ &= -\boldsymbol{u}_N^T[A(t)][A(t)]^\dagger\boldsymbol{u}_N = -\boldsymbol{u}_N^T\boldsymbol{\alpha}_N \leq 0 \end{aligned} \quad (21)$$

If it can be shown that $[A][A]^\dagger$ is a positive semi-definite matrix, then Eq. (21) shows that $\dot{V} \leq 0$ and the charging control is uniformly stabilizing.

To show that $[A][A]^\dagger$ is positive semi-definite, the singular value decomposition (SVD) is applied to the $[A]$ matrix.

$$[A(t)] = [U(t)][D(t)][V(t)]^T \quad (22)$$

where $[U]$ is a 3×3 orthonormal matrix, $[V]$ is a $L\times L$ orthonormal matrix, and the $3\times L$ matrix $[D]$ contains the singular values of $[A]$ in a diagonal form.

$$[D(t)] = \begin{bmatrix}\sigma_1(t) & 0 & 0 & \cdots & 0\\ 0 & \sigma_2(t) & 0 & \cdots & 0\\ 0 & 0 & \sigma_3(t) & \cdots & 0\end{bmatrix} \quad (23)$$

The typical convention is assumed here where $\sigma_1 \geq \sigma_2 \geq \sigma_3$. For notational convenience, the explicit time dependence notation is dropped from here on. If $[A]$ has rank 1, then $\sigma_2 = \sigma_3 = 0$. If $[A]$ has rank 2, then only $\sigma_3 = 0$. If $[A]$ has full rank, then all three σ_i values will be non-zero. The pseudo-inverse of a matrix is defined using the SVD as

$$[A]^\dagger = [V][D]^\dagger[U]^T \quad (24)$$

The pseudo-inverse of $[D]$ is defined as

$$[D]^\dagger = \begin{bmatrix}1/\sigma_1 & 0 & 0\\ 0 & 1/\sigma_2 & 0\\ 0 & 0 & 1/\sigma_3\\ \vdots & \vdots & \vdots\\ 0 & 0 & 0\end{bmatrix} \quad (25)$$

where the $1/\sigma_i$ entries are set to zero if $\sigma_i = 0$.

Since a matrix is positive semi-definite if all its eigenvalues are greater than or equal to zero, the eigenvalue/eigenvector problem of the 3×3 matrix $[A][A]^\dagger$ is investigated. Let $[\mathcal{V}]$ be a matrix of eigenvectors of $[A][A]^\dagger$ and $[\Lambda]$ be the corresponding diagonal eigenvalue matrix.

$$[A][A]^\dagger = [\mathcal{V}][\Lambda][\mathcal{V}]^T \qquad \text{or} \qquad [A][A]^\dagger[\mathcal{V}] = [\mathcal{V}][\Lambda] \quad (26)$$

must be true. Let's assume that $[\mathcal{V}] = [U]$. Then

$$[A][A]^\dagger[U] = [U][D][V]^T[V][D]^\dagger[U]^T[U] = [U][D][D]^\dagger \quad (27)$$

must be true. This shows that $[U]$ is indeed the eigenvector matrix of $[A][A]^\dagger$ and that the matrix $[\Lambda] = [D][D]^\dagger$ is the corresponding diagonal eigenvalue matrix. Using Eqs. (23) and (25), we find that

$$[D][D]^\dagger = \begin{bmatrix}1 & 0 & 0\\ 0 & i & 0\\ 0 & 0 & j\end{bmatrix} \qquad \text{with } i, j = 0, 1 \quad (28)$$

If the rank of $[A]$ is 2, then j = 0. If the rank of $[A]$ is 1, then $i = j = 0$. Since $[D][D]^\dagger$ is the eigenvalue matrix of $[A][A]^\dagger$, it has been shown that the eigenvalues of $[A][A]^\dagger$ are either 1 or zero, depending on the rank of the $[A]$ matrix. Thus, the matrix $[A][A]^\dagger$ is positive semi-definite and the Lyapunov rate function expression in Eq. (21) is indeed non-positive with $\dot{V} \leq 0$. This shows that the projection used to compute the charging products Q_{iN} will yield a globally stabilizing feedback control law for the tracking errors of the N-th satellite. Note that the issue of convergence will be addressed later on. Another useful property of $[A][A]^\dagger$ is that

$$[A][A]^\dagger = \left([A][A]^\dagger\right)^T \quad (29)$$

Also, note that the self-similarity property yields

$$\begin{aligned}([A][A]^\dagger)([A][A]^\dagger) &= [U][D][D]^\dagger[U]^T[U][D][D]^\dagger[U]^T \\ &= [U][D][D]^\dagger[U]^T = ([A][A]^\dagger) \end{aligned} \quad (30)$$

since $([D][D]^\dagger)([D][D]^\dagger) = [D][D]^\dagger$.

The proof shown only guarantees stability for controlling the tracking error of the N-th satellite (the one with the worst tracking error). If this orbit correction causes another satellite to have a worse tracking error, then the structured control law will switch to use the remaining satellites to control this new "worst" satellite. If the spacecraft charging ability is unlimited, then this control technique will attempt to iteratively stabilize all the satellite tracking errors.

Saturated Control Stability Analysis

In any practical application of CSF, the craft charge q_i will be limited to finite values. Large electrostatic potential could lead to a differential discharge that could damage on board electronics and sensors. Let

$$|q_i| \leq q_{i,\max} \quad (31)$$

Then the charge products Q_{iN} are limited to

$$|Q_{iN}| \leq q_{i,\max}\, q_{N,\max} = Q_{iN,\max} \quad (32)$$

The saturated charge product term $\tilde{Q_{iN}}$ is then defined to be

$$\tilde{Q}_{iN} = \begin{cases} -Q_{iN,\max} & \text{if} \quad Q_{iN} < -Q_{iN,\max} \\ Q_{iN} & \text{if} \quad -Q_{iN,\max} \leq Q_{iN} \leq Q_{iN,\max} \\ Q_{iN,\max} & \text{if} \quad Q_{iN} > Q_{iN,\max} \end{cases} \quad (33)$$

Note that

$$\boldsymbol{Q}^T\tilde{\boldsymbol{Q}} = Q_{1N}\tilde{Q}_{iN} + \cdots + Q_{LN}\tilde{Q}_{LN} \geq 0 \quad (34)$$

Next, let's investigate how applying saturated spacecraft charges will affect the previous stability proof. Note that the saturation function in Eq. (33) allows for each craft to have a different electrical charge saturation limit. The acceleration vector $\boldsymbol{\alpha}_N$ due to saturated spacecraft charges is

$$\boldsymbol{\alpha}_N = \frac{k_c}{m_N}[A]\tilde{\boldsymbol{Q}} \quad (35)$$

Using Eqs. (14) and (18), we can express the ideal control acceleration vector $\boldsymbol{u}_N$ in terms of the unsaturated charge vector $\boldsymbol{Q}$.

$$\boldsymbol{u}_N = \frac{k_c}{m_N}\left([A][A]^\dagger\right)^\dagger[A]\boldsymbol{Q} \quad (36)$$

Note that the pseudo-inverse of the 3×3 matrix $\left([A][A]^\dagger\right)$ is simply $\left([A][A]^\dagger\right)$. This can be shown by using Eq. (30) to find that $\left([A][A]^\dagger\right) = [U]([D][D]^\dagger)[U]^T$, and thus

$$\begin{aligned}\left([A][A]^\dagger\right)^\dagger &= [U]([D][D]^\dagger)^\dagger[U]^T \\ &= [U]([D][D]^\dagger)[U]^T = \left([A][A]^\dagger\right) \end{aligned} \quad (37)$$

since $([D][D]^\dagger)^\dagger = ([D][D]^\dagger)$. Using Eqs. (35)–(37), the Lyapunov rate function in Eq. (21) is expressed as

$$\dot{V} = -\boldsymbol{u}_N^T\boldsymbol{\alpha}_N = -\frac{k_c^2}{m_N^2}\boldsymbol{Q}^T[A]^T\left([A][A]^\dagger\right)[A]\tilde{\boldsymbol{Q}} \quad (38)$$

Using Eq. (22) and the orthogonality properties of the matrices $[U]$ and $[V]$, the term $[A]^T\left([A][A]^\dagger\right)[A]$ can be written as

$$\begin{aligned}&[A]^T\left([A][A]^\dagger\right)[A] \\ &\quad = [V][D]^T[U]^T[U][D][V]^T[V][D]^\dagger[U]^T[U][D][V]^T \\ &\quad = [V][D]^T\left([D][D]^\dagger\right)[D][V]^T \end{aligned} \quad (39)$$

Using Eqs. (23) and (28) we find that the diagonal $L \times L$ matrix is

$$[D]^T \left([D][D]^\dagger \right) [D] = \begin{bmatrix} \sigma_1^2 & 0 & 0 & \cdots & 0 \\ 0 & \sigma_2^2 & 0 & \cdots & 0 \\ 0 & 0 & \sigma_3^2 & \cdots & 0 \\ \vdots & \vdots & \vdots & \ddots & \vdots \\ 0 & 0 & 0 & \cdots & 0 \end{bmatrix} \tag{40}$$

where $\sigma_3 = 0$ if rank($[A]$) = 2 and $\sigma_2 = \sigma_3 = 0$ if rank($[A]$) = 1. With this convention, the following development is applicable regardless of the rank of the matrix $[A]$. Next, the $L \times L$ orthogonal matrix $[V]$ is written as

$$[V] = [\boldsymbol{v}_1 \quad \boldsymbol{v}_2 \quad \boldsymbol{v}_3 \quad \cdots \quad \boldsymbol{v}_L] \tag{41}$$

where $\boldsymbol{v}_i$ is the L-dimensional column vector of $[V]$. Using Eqs. (39) – (41), the Lyapunov rate function in Eq. (38) is expressed as

$$\dot{V} = -\frac{k_c^2}{m_N^2} \boldsymbol{Q}^T \left(\sigma_1^2 \boldsymbol{v}_1 \boldsymbol{v}_1^T + \sigma_2^2 \boldsymbol{v}_2 \boldsymbol{v}_2^T + \sigma_3^2 \boldsymbol{v}_3 \boldsymbol{v}_3^T \right) \tilde{\boldsymbol{Q}} \tag{42}$$

Rearranging this equation, the Lyapunov rate function with saturated spacecraft charging is finally expressed as

$$\dot{V} = -\frac{k_c^2}{m_N^2} \left(\sigma_1^2 \boldsymbol{v}_1^T \boldsymbol{Q} \tilde{\boldsymbol{Q}}^T \boldsymbol{v}_1 + \sigma_2^2 \boldsymbol{v}_2^T \boldsymbol{Q} \tilde{\boldsymbol{Q}}^T \boldsymbol{v}_2 + \sigma_3^2 \boldsymbol{v}_3^T \boldsymbol{Q} \tilde{\boldsymbol{Q}}^T \boldsymbol{v}_3 \right) \tag{43}$$

If it can be shown that the $L \times L$ matrix $\boldsymbol{Q}\tilde{\boldsymbol{Q}}^T$ is positive semi-definite, then $\dot{V} \leq 0$ and the saturated charging control law is globally, uniformly stabilizing. Note that this stability statement is valid regardless of the rank of the $[A]$ matrix. If $[A]$ is not full rank, then σ_3 and/or σ_2 will be zero, but the $\dot{V}$ function will remain non-positive through-out these cases.

The matrix $\boldsymbol{Q}\tilde{\boldsymbol{Q}}^T$ is positive semi-definite if its eigenvalues are non-negative. Since $\boldsymbol{Q}\tilde{\boldsymbol{Q}}^T$ will only have rank 1, there will be a single non-zero eigenvalue λ. Let $\boldsymbol{v}$ be the associated eigenvector. Then the eigenvalue problem is solved by studying the equation

$$\left(\boldsymbol{Q}\tilde{\boldsymbol{Q}}^T \right) \boldsymbol{v} = \lambda \boldsymbol{v} \tag{44}$$

Note that

$$\left(\boldsymbol{Q}\tilde{\boldsymbol{Q}}^T \right) \boldsymbol{Q} = \boldsymbol{Q}(\tilde{\boldsymbol{Q}}^T \boldsymbol{Q}) = (\tilde{\boldsymbol{Q}}^T \boldsymbol{Q}) \boldsymbol{Q} \tag{45}$$

Thus the non-zero eigenvalue of $\boldsymbol{Q}\tilde{\boldsymbol{Q}}^T$ and associated eigenvector must be

$$\lambda = \boldsymbol{Q}^T \tilde{\boldsymbol{Q}} \tag{46}$$

$$\boldsymbol{v} = \boldsymbol{Q} \tag{47}$$

Due to the saturation function property in Eq. (34), we find that the eigenvalue $\lambda > 0$ and thus the matrix $\boldsymbol{Q}\tilde{\boldsymbol{Q}}^T$ is positive semi-definite. In return, this guarantees that $\dot{V} \leq 0$ in Eq. (43), and the saturated charging control law is globally, uniformly stabilizing. Note that convergence issues have not been addressed here. Further, this control law only guarantees that the tracking error dynamics of the N-th satellite will be stable. If two neighboring satellites repel each other while correcting this N-th satellite, then it is possible that they could receive enough energy such that the *saturated* charging control law would not be able to stabilize their tracking error. Currently the structured control law will simply attempt to correct the satellite with the worst tracking errors, and use the remaining satellite charges to do so. Future work on these charging control laws will investigate this issue as well when computing the spacecraft charge product vector $\boldsymbol{Q}$ in Eq. (15).

Convergence of Semi-Major Axis Only Control

Up to this point the spacecraft charging control law is written to stabilize any set of orbit element tracking errors. From here on, the focus is to control only the semi-major axis tracking errors. If Keplerian orbital motion is assumed, then the semi-major axes of all spacecraft must be equal in order to obtain bounded relative motion between the satellites. Asymptotic stability of a semi-major axis specific control law has already been shown for the two-satellite special case in the previous development in Reference 7. Convergence of the semi-major axes tracking errors is crucial to keep the CSF relative motion bounded. For example, if the spacecraft form a swarm, rather than a precise formation, it could be sufficient to keep the cluster of spacecraft on bounded relative orbits. Note that collision avoidance is not being addressed here and is a topic of future work.

If only the semi-major axis tracking error is controlled with $\delta\boldsymbol{\epsilon} \approx \delta a$, then the tracking error dynamics in Eq. (7) reduces to

$$\delta \dot{a}_N = [B(t)]\boldsymbol{\alpha}_N = \underbrace{\frac{2a^2}{h} \begin{bmatrix} e \sin f(t) & (1 + e\cos f(t)) & 0 \end{bmatrix}}_{[B]} \boldsymbol{\alpha}_N \tag{48}$$

where a is the semi-major axis, h is the angular momentum, e is the eccentricity, p is the semi-latus rectum, f is the true anomaly angle and r is the orbit radius of the chief orbit (barycenter position of the formation). Note that charge saturation is not modeled in this convergence analysis. The ideal control acceleration vector is written as

$$\boldsymbol{u}_N = -[B(t)]^T K \delta a \tag{49}$$

where the gain matrix $[K]$ has been replaced with a scalar positive parameter K. The corresponding unsaturated charging control law is

$$\boldsymbol{Q} = -\frac{m_N}{k_c} [A(t)]^\dagger [B(t)]^T K \delta a \tag{50}$$

The Lyapunov function simplifies for the semi-major axis only control case to

$$V(\delta a_N) = \frac{K}{2} \delta a_N^2 \tag{51}$$

Using the error dynamics in Eq. (48), the unsaturated Lyapunov rate expression in Eq. (21) simplifies to

$$\dot{V} = -\delta a_N^2 K^2 \left([B(t)][A(t)][A(t)]^\dagger [B(t)]^T \right) \tag{52}$$

This expression can be further simplified using the $3 \times L$ matrix $[C]$ and $L \times L$ matrix $[S]$ by defining

$$[A] = [C][S] \tag{53}$$

$$[C] = [\hat{\boldsymbol{r}}_{1N} \quad \cdots \quad \hat{\boldsymbol{r}}_{LN}] \tag{54}$$

$$[S] = \begin{bmatrix} \frac{1}{r_{1N}^2} & \cdots & 0 \\ \vdots & \ddots & \vdots \\ 0 & \cdots & \frac{1}{r_{LN}^2} \end{bmatrix} \tag{55}$$

Note that the pseudo-inverse of $[A]$ can now be written as

$$[A]^\dagger = [S]^\dagger [C]^\dagger = [S]^{-1} [C]^\dagger \tag{56}$$

which allows the Lyapunov rate to be expressed as

$$\dot{V} = -\delta a_N^2 K^2 \left([B(t)][C(t)][C(t)]^\dagger [B(t)]^T \right) \tag{57}$$

Note that if rank($[A]$) = rank($[C]$) = 3, then $[C][C]^\dagger = [I_{3\times 3}]$ and the Lyapunov rate function is

$$\dot{V} = -\delta a_N^2 K^2 \left([B][B]^T \right) \tag{58}$$

This function has already been shown to be negative definite in the tracking errors δa in Reference 9–12, and thus the full rank $[A]$ matrix case is asymptotically stabilizing. The following development will show that $\boldsymbol{Q}$ in Eq (50) is asymptotically stabilizing, regardless of the rank of $[A(t)]$.

Proving asymptotic converge for an non-autonomous system is more involved than for autonomous systems. For example, if it could be shown that[14,15]

$$-\dot{V}(\delta a_N, t) \geq W_3(\delta a_N) \tag{59}$$

where $W_3(\delta a_N)$ is a positive definite function, then the system would be asymptotically stabilizing. This was attempted by expressing the $[C]$ matrix using a linearized orbital relative motion solution[16] for the rank($[A]$) $= 1$ case. However, this analysis showed that such a W_3 function cannot exist for the given $\dot{V}$ expression in Eq. (57). Instead, let us investigate $\dot{V}$ as $t \to \infty$. If V has a finite limit, and $\dot{V}$ is uniformly continuous, then Barbalat's lemma[14,15] states that $\dot{V} \to 0$. Because the control has already been shown to be stabilizing, the Lyapunov function V will have a finite limit. To show that $\dot{V}$ is uniformly continuous, it is sufficient to show that $\ddot{V}$ is bounded.[14] Taking the derivative of the $\dot{V}$ expression in Eq. (57) and using Eq. (48), we find

$$\begin{aligned}\ddot{V} = &-2\delta a_N^2 K^3 \Big([B][C][C]^\dagger[B]^T\Big)^2 \\ &- \delta a_N^2 K \Big([\dot{B}][C][C]^\dagger[B]^T + [B][\dot{C}][C]^\dagger[B]^T \\ &+ [B][C][\dot{C}]^\dagger[B]^T + [B][C][C]^\dagger[\dot{B}]^T\Big)\end{aligned} \tag{60}$$

Because the charge control in Eq. (50) is stabilizing, we find that δa_N will be finite. The matrix $[B]$ formulation in Eq. (48) is clearly bounded for all $f(t)$, and will have continuous, finite derivatives $[\dot{B}]$ because orbital dynamics dictates that $\dot{f} = \frac{h}{p^2}(1 + e\cos f)^2$. The $[C]$ matrix is constructed using unit direction vectors of the relative position vectors $\boldsymbol{r}_{iN}$, and thus is always bounded. The $[\dot{C}]$ matrix will depend on the $\dot{\boldsymbol{r}}_{iN}$ vectors. These are also a finite quantities, even if the charges have discrete jumps in their values. Thus $\dot{V}$ is found to be uniformly continuous, and $\dot{V} \to 0$. Looking at Eq. (57), $\dot{V} = 0$ is only possible if either $\delta a_N = 0$, or $[B][C][C]^\dagger[B]^T$ is zero.

Let us rewrite the Lyapunov rate expression $\dot{V}$ into a more convenient form. Taking the SVD of $[C]$ we find

$$[C] = [U_c][D_c][V_c]^T \tag{61}$$

where $[U_c]$ is a 3×3 orthogonal matrix, $[D_c]$ is a $3 \times L$ diagonal matrix, and $[V_c]$ is a $L \times L$ orthogonal matrix. The matrix product $[C][C]^\dagger$ is written as

$$\begin{aligned}[C][C]^\dagger &= [U_c][D_c][V_c]^T[V_c][D_c]^\dagger[U_c] \\ &= [U_c][D_c][D_c]^\dagger[U_c] \\ &= [U_c]\begin{bmatrix}\delta_1 & 0 & 0\\ 0 & \delta_2 & 0\\ 0 & 0 & \delta_3\end{bmatrix}[U_c]^T\end{aligned} \tag{62}$$

where

$$\delta_i = \begin{cases}1 & \text{if } i \leq \text{rank}([C])\\ 0 & \text{else}\end{cases} \tag{63}$$

Let the 3×3 matrix $[U_c]$ be partitioned into three column vectors $\boldsymbol{u}_{c_i}$.

$$[U_c] = [\boldsymbol{u}_{c_1} \quad \boldsymbol{u}_{c_2} \quad \boldsymbol{u}_{c_3}] \tag{64}$$

Eq. (62) can now be written as

$$[C][C]^\dagger = \delta_1 \boldsymbol{u}_{c_1}\boldsymbol{u}_{c_1}^T + \delta_2 \boldsymbol{u}_{c_2}\boldsymbol{u}_{c_2}^T + \delta_3 \boldsymbol{u}_{c_3}\boldsymbol{u}_{c_3}^T \tag{65}$$

Substituting Eq. (65) into Eq. (57) and rearranging the terms, the Lyapunov rate function is expressed for the semi-major axis only control law as

$$\dot{V} = -\delta a_N^2 K^2\big(\delta_1([B]\boldsymbol{u}_{c_1})^2 + \delta_2([B]\boldsymbol{u}_{c_2})^2 + \delta_3([B]\boldsymbol{u}_{c_3})^2\big) \tag{66}$$

If it can be shown that the $[B]\boldsymbol{u}_{c_i}$ terms cannot remain zero for non-zero δa terms, then asymptotic convergence of the semi-major axis only CSF charging control law has been shown. Let's write $[B]^T = \boldsymbol{b}$ as a column vector. Using the $[B]$ definition in Eq. (48), it is clear that $\boldsymbol{b}$ cannot be a zero vector. Then Eq. (66) is written as

$$\dot{V} = -\delta a_N^2 K^2 \left(\delta_1(\boldsymbol{b}\cdot\boldsymbol{u}_{c_1})^2 + \delta_2(\boldsymbol{b}\cdot\boldsymbol{u}_{c_2})^2 + \delta_3(\boldsymbol{b}\cdot\boldsymbol{u}_{c_3})^2\right) \tag{67}$$

Let us re-write the charging vector expression in Eq. (50) using Eqs. (53), (61) and (64).

$$\begin{aligned}\boldsymbol{Q} &= -\frac{m_N}{k_c}[A]^\dagger[B]^T K\delta a_N \\ &= -\frac{m_N}{k_c}K\delta a_N[S]^{-1}[C]^\dagger[B]^T \\ &= -\frac{m_N}{k_c}K\delta a_N[S]^{-1}[V_c][D_c]^\dagger[U_c]^T[B]^T \\ &= -\frac{m_N}{k_c}K\delta a_N[S]^{-1}[V_c][\text{diag}(1/\sigma_{c_i})][U_c]^T[B]^T \\ &= -\frac{m_N}{k_c}K\delta a_N[S]^{-1}[V_c][\text{diag}(1/\sigma_{c_i}\boldsymbol{b}\cdot\boldsymbol{u}_{c_i})]\end{aligned} \tag{68}$$

The positive scalars σ_{c_i} are the singular values of $[C]$ and the diagonal entries of $[D_c]$. The $L \times 3$ matrix $[\text{diag}(1/\sigma_{c_i})]$ has diagonal matrix on the upper 3×3 partition, and zeros on the lower $(L-3)\times 3$ partition. Note that if the Lyapunov rate $\dot{V}$ in Eq. (67) is zero due to $\boldsymbol{b}\cdot\boldsymbol{u}_{c_i}$ terms being zero, then the charge product vector $\boldsymbol{Q}$ will also be zero. From this observation it can be concluded that if $\dot{V}$ goes to zero with $\delta a_N \neq 0$, then all spacecraft charges will also have gone to zero and the relative motion will be determined purely through the orbital mechanics. Thus, to discuss convergence of $\delta a_N \to 0$, it must be investigated if it is possible for $\boldsymbol{b}\cdot\boldsymbol{u}_{c_i}$ to be zero with the uncontrolled relative orbit motion.

First, assume that rank($[C]$) $= 3$ and $\delta_1 = \delta_2 = \delta_3 = 1$. In this case it is impossible for $\dot{V}$ in Eq. (67) to be zero for a non-zero δa_N. If $\boldsymbol{b}$ is perpendicular to both $\boldsymbol{u}_{c_1}$ and $\boldsymbol{u}_{c_2}$, then due to the orthogonality of the $\boldsymbol{u}_{c_i}$ vectors, the $\boldsymbol{b}$ vector cannot be orthogonal to $\boldsymbol{u}_{c_3}$. Thus, for the full rank case of either $[C]$ or $[A]$, the semi-major axis only charging control law is shown to be asymptotically stabilizing. Note that for this full rank case the formation chief orbit can be either circular or elliptic in nature.

To prove asymptotic convergence for a matrix $[A]$ without full rank is more challenging. Let's first investigate the case where rank($[A]$) = rank($[C]$) $= 1$. This could be a situation where only two satellites are in a cluster, or all satellite relative position vectors happen to be collinear. Here $\delta_1 = 1$ and $\delta_2 = \delta_3 = 0$, and thus

$$\dot{V} = -\delta a_N^2 K^2(\boldsymbol{b}\cdot\boldsymbol{u}_{c_1})^2 \tag{69}$$

Without loss of generality, assume that $N = 2$ here and $[C] = [\hat{\boldsymbol{r}}_{1N}]$. Here the SVD of $[C]$ is

$$[C] = \underbrace{[\hat{\boldsymbol{r}}_{1N} \quad \boldsymbol{u}_{c_2} \quad \boldsymbol{u}_{c_3}]}_{[U_c]}\underbrace{\begin{bmatrix}1\\0\\0\end{bmatrix}}_{[D_c]}\underbrace{[1]^T}_{[V_c]^T} \tag{70}$$

and $\boldsymbol{u}_{c_1} = \hat{\boldsymbol{r}}_{1N} = (\hat{\rho}_1, \hat{\rho}_2, \hat{\rho}_3)^T$. For the term $\boldsymbol{b}\cdot\boldsymbol{u}_{c_1}$ to be zero, the condition

$$\boldsymbol{b}\cdot\boldsymbol{u}_{c_1} \simeq \hat{\rho}_1 e\sin f + \hat{\rho}_2\frac{p}{r} = 0 \tag{71}$$

must be true. Note that proportionality factors have been dropped in this expression for convenience. If $\boldsymbol{b}\cdot\boldsymbol{u}_{c_1} = 0$, then $\boldsymbol{Q} = 0$. Thus, a natural orbital motion must be found that could satisfy the constraint in Eq. (71) for $\boldsymbol{b}\cdot\boldsymbol{u}_{c_1} = 0$ to be true. Reference 16

provides a convenient relative orbit description in terms of classical orbit element differences:

$$\hat{\rho}_1 \simeq \frac{r}{a}\delta a + \frac{ae\sin f}{\eta}\delta M - a\cos f\delta e \tag{72}$$

$$\hat{\rho}_2 \simeq \frac{r}{\eta^3}(1+e\cos f)^2\delta M + r\delta\omega + \frac{r\sin f}{\eta^2}(2+e\cos f)\delta e + r\cos i\delta\Omega \tag{73}$$

where ω is the argument of periapses, Ω is the ascending node, $\eta = \sqrt{1-e^2}$ being an eccentricity measure, and M is the mean anomaly angle of the formation chief orbit. For small relative orbits, the linearized mean anomaly difference will evolve according to[16]

$$\delta M(f) = \delta M_0 - \frac{3}{2}\left(M(f) - M_0\right)\frac{\delta a}{a} \tag{74}$$

For the condition in Eq. (71) to be true for all time, it is necessary that the secular terms must vanish independently. If $\delta a \neq 0$, then we can treat the mean anomaly differences δM as secularly growing terms in Eqs. (72) and (73) without loss of generality. Ignoring the constant and cyclic terms in $\hat{\rho}_1$ and $\hat{\rho}_2$, we focus on studying the effect of the secular δM terms on the constraint in Eq. (71).

$$(e\sin f)\left(\frac{ae\sin f}{\eta}\delta M\right) + \frac{p}{r}\left(\frac{r}{\eta^3}(1+e\cos f)^2\delta M\right) \simeq 0 \tag{75}$$

Using the orbit radius equation $r = p/(1+e\cos f)$ and $p = a\eta^2$, the constraint is written as

$$\left(1+e^2+2e\cos f\right)\delta M \simeq 0 \tag{76}$$

For this expression to be zero, the true anomaly angle f would have to satisfy

$$\cos f = -\frac{1+e^2}{2e} \tag{77}$$

Note that this equation will only yield a real answer for f if $e = 1$. Thus, for circular orbits where $e = 0$ and non-rectilinear elliptic orbits where $e < 1$, the constraint in Eq. (71) can never be satisfied with a non-zero δa and thus $\boldsymbol{b}\cdot\boldsymbol{u}_{c_1}$ cannot remain zero. If fact, this shows that $\boldsymbol{b}$ cannot remain orthogonal to the relative position vectors $\boldsymbol{r}_{iN}$. Having shown this for the secular terms in Eq. (71), there is no need to investigate the periodic terms. The semi-major axis only charging control law is thus asymptotically stabilizing for the case where rank($[A]$) = 1. Note that with the two-spacecraft case studied in Reference 7, asymptotic convergence was only analytically shown for the circular chief orbit case. The above analysis extends this analytic proof to elliptic orbits and a larger number of spacecraft.

If the matrix $[A]$ has a rank of 2 (all relative position vectors lie in a common plane), then $\delta_1 = \delta_2 = 1$ and $\delta_3 = 0$. The Lyapunov rate expression in Eq. (67) is now given by

$$\dot{V} = -\delta a_N^2 K^2\left(\left(\boldsymbol{b}\cdot\boldsymbol{u}_{c_1}\right)^2 + \left(\boldsymbol{b}\cdot\boldsymbol{u}_{c_2}\right)^2\right) \tag{78}$$

If the vector $\boldsymbol{b} = [B]^T$ is in the plane described by the vector pair $\boldsymbol{u}_{c_1}$ and $\boldsymbol{u}_{c_2}$, then the orthogonality of the $\boldsymbol{u}_{c_i}$ vectors guarantees that the Lyapunov rate function in Eq. (78) cannot be zero for a non-zero δa. The only possibility for $\left(\left(\boldsymbol{b}\cdot\boldsymbol{u}_{c_1}\right)^2 + \left(\boldsymbol{b}\cdot\boldsymbol{u}_{c_2}\right)^2\right)$ to be zero is for $\boldsymbol{b}$ to be perpendicular to the plane described by the vector pair $\boldsymbol{u}_{c_1}$ and $\boldsymbol{u}_{c_2}$. Recall the rank($[A]$) = 1 case, where we found that $\boldsymbol{u}_{c_1} = \hat{\boldsymbol{\rho}}_{1N}$. This is generally not the case when rank($[A]$) = 2. However, the orthogonal $\boldsymbol{u}_{c_1}$ and $\boldsymbol{u}_{c_2}$ vectors will span the plane described by the relative position vectors $\boldsymbol{r}_{iN}$. For $\dot{V}$ in Eq. (78) to not be zero with $\delta a_N \neq 0$, the vector $\boldsymbol{b}$ cannot remain orthogonal to both $\boldsymbol{u}_{c_1}$ and $\boldsymbol{u}_{c_2}$. This implies that $\boldsymbol{b}$ cannot remain orthogonal to the orbit plane described through $\boldsymbol{u}_{c_1}$ and $\boldsymbol{u}_{c_2}$, and thus $\boldsymbol{b}$ cannot remain orthogonal to any of the relative position vectors $\boldsymbol{r}_{iN}$ which lie in this relative orbit plane. However, while studying the rank($[A]$) = 1 case, it was shown that $\boldsymbol{b}$ cannot remain orthogonal to the relative position vectors. Thus, we can conclude that $\dot{V}$ in Eq. (78) cannot remain zero unless δa_N = 0. Combining all rank cases of the matrix $[A]$, we find that the charge control law in Eq. (50) will indeed asymptotically stabilize the δa_N tracking errors for all rank cases of $[A]$.

Numerical Simulation

A numerical simulation is used to illustrate the performance of the saturated spacecraft charging control law in Eqs. (15) and (33). The only orbit element being controlled here is the semi-major axis. The control attempts to set all osculating semi-major axes to equal values. The structured control strategy is to find the satellite with the worst semi-major axis tracking error (controlled satellite labeled N) and use the remaining satellites to correct this error (non-controlled satellites). If the tracking error of another satellite increases enough to become the largest tracking error of the formation, then this satellite becomes the controlled satellite. Note that no stability guarantees have been provided for this simple switching strategy. However, the following numerical illustration does illustrate that it can be used to control the semi-major axis errors of a 3 spacecraft formation, and not just control the tracking error of a single satellite within this formation. To avoid excessive chattering through switching between two satellites with nearly equal tracking errors, a minimum wait time of 60 seconds is introduced before the controlled satellite label is switched.

The CSF consists of three satellites. The initial Keplerian elements and the masses of the satellites are shown in Table 1. The highly elliptic orbits have an apoapses radius of about 10 Earth radii, while the periapses radius is about 3.3 Earth radii. Highly elliptical missions are envisioned to study the tail of Earth's magnetosphere. A cluster of Coulomb spacecraft could provide local gradient measurements. Note that while typical cluster or formation concepts contain craft of similar build, this simulation assumes the craft have widely differing masses to illustrate the stability of the control in this situation. Note the different semi-major axes of each satellite. Even these small differences would cause the uncontrolled satellites to drift apart by 100's of meters per orbit.

The numerical simulation integrates the inertial differential equations motion (Eq. (1)) of each craft including the J_2–J_5 gravitational effects. A Debye length value of λ_d = 1000 meters is modeled. The satellite electrical charging is limited to magnitudes less than $q_{\max} = 1\mu$C. This is a rather small, conservative charge limit. Because the current control strategy doesn't avoid charging two non-controlled craft in close proximity, which could result in these two craft strongly attracting or repelling each other, having this lower saturation limit helps in avoiding the non-controlled spacecraft bursting apart.

Figure 1 illustrates the resulting spacecraft charge time histories and the semi-major axis tracking errors relative to the formation center of mass motion (chief motion). The saturated charging control law is able to stabilize the semi-major axis tracking errors and drives them to zero. Due to the J_2–J_5 perturbations, small tracking errors do occur and are periodically corrected by the spacecraft charges. Numerical studies show that the space plasma Debye length can have an effect on the convergence rate of the control law, because the effectiveness of the Coulomb charge is reduced. However, stability is still retained in the cases studied.

The three-dimensional relative motion of the various satellites about the orbit position (formation barycenter position) is illustrated in Figure 2. In particular, Figure 2(a) shows how the relative orbit will pull apart in the along-track direction due to the initial semi-major axis differences if no control is applied. Within the three orbit periods shown, the along-track relative motion has already grown to nearly 400 meters. In contrast, Figure 2(b) shows the relative motion if the charging control is applied. Here the semi-major axes become equal, which results in all orbits having the same period, and the relative motions remain bounded over time.

The stability proofs in this paper address the situation where the tracking errors of a single satellite are controlled through the Coulomb charges of the remaining satellites. The simulation

Table 1 Satellite Simulation Data

	Satellite 1	Satellite 2	Satellite 3	Units
semi-major axis a	42241.075	42241.089	42241.088	km
eccentricity e	0.500000	0.5000007	0.5000009	
inclination i	48.00000	48.00000	48.00010	deg
ascending node Ω	20.00000	20.00005	19.99995	deg
argument of perigee ω	0.00000	0.00002	0.00000	deg
initial mean anomaly M_0	20.00000	20.00000	20.00005	deg
mass m	150.000	50.000	110.000	kg

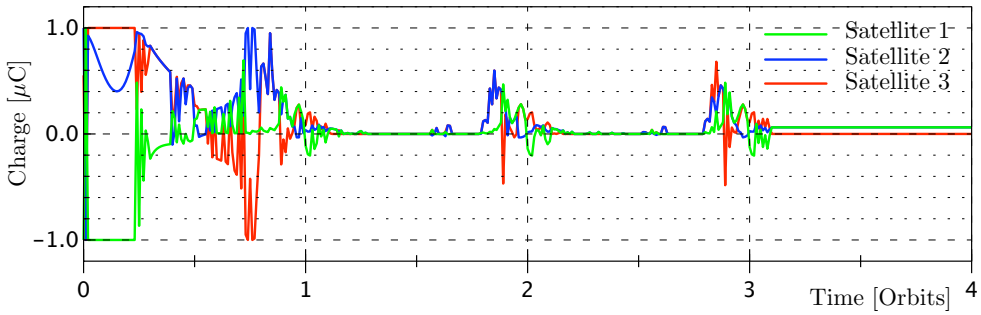

a) Spacecraft Charging

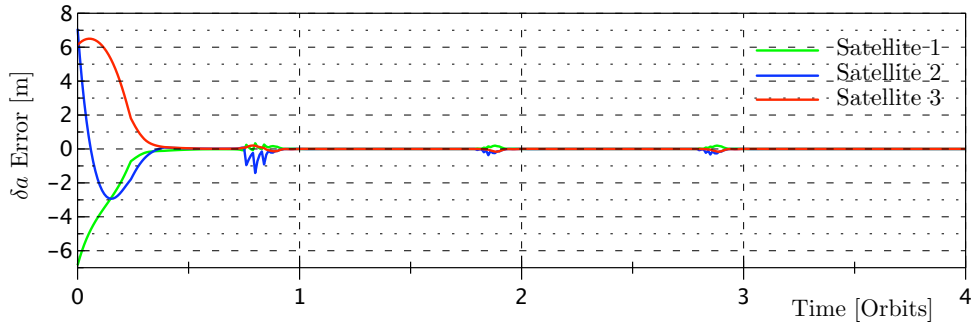

b) Semi-Major Axes Tracking Errors

Fig. 1 Control Charge and Tracking Error Results of the Numerical Simulation.

shown extends this control strategy to stabilize the semi-major axis of all formation satellites through a switching structure. This strategy appears to work reasonably with three satellites, but not without issues as discussed earlier. Numerical simulations of formations with more than 3 satellites often showed convergence issues where the formation size grows so large that the electrical charges no longer are effective in controlling the relative motion. Refined structured control methods will need to be developed to more robustly be able to stabilize the relative motion of larger satellite clusters using only Coulomb forces.

Conclusions

A stabilizing spacecraft charging control law is investigated. While previous work looked at correcting the orbit of one satellite by electrically pushing and pulling on another satellite (2-satellite formation with equal mass), this paper studies the more general N-body formation with unequal masses and individual electrical charging limits. Using an orbit element difference formulation to describe and control the relative motion, global stability of the charging control law is shown for both unsaturated and saturated charging cases. The general version of the control can be applied to controlling any set of orbit element differences relative to the formation chief or center of mass motion. However, a special case of this control is investigated further for convergence properties, where only the semi-major axes of the Coulomb satellites are controlled. This control is able to bound the relative motion of a satellite relative to the chief motion and cancel secular drift. To control the semi-major axes of all the satellites in the formation, a simple structured control approach is investigated. Here only the satellite with the worst tracking error is corrected, and the remaining satellites are used to achieve this. All stability claims shown are only valid for controlling the relative motion of the satellite with the worst tracking errors. No stability claims are provided for the other satellites. Numerical simulations show that this strategy can function to bound the relative motion of a three-satellite formation using only Coulomb charges as the control mechanism. However, to control a larger formation, a more sophisticated structured control approach would be needed.

Acknowledgment

I would like to thank Dr. G. G. Parker and Dr. L. B. King at Michigan Tech for helpful discussions on Coulomb satellite formations that lead to an enhanced version of this paper.

References

[1]Mullen, E. G., Gussenhoven, M. S., and Hardy, D. A., "SCATHA Survey of High-Voltage Spacecraft Charging in Sunlight," *Journal of the Geophysical Sciences*, Vol. 91, 1986, pp. 1074–1090.

[2]King, L. B., Parker, G. G., Deshmukh, S., and Chong, J.-H., "Spacecraft Formation-Flying using Inter-Vehicle Coulomb Forces," Tech. report, NASA/NIAC, January 2002, `http://www.niac.usra.edu`.

[3]King, L. B., Parker, G. G., Deshmukh, S., and Chong, J.-H., "Study of Inter-spacecraft Coulomb Forces and Implications for Formation Flying," *AIAA Journal of Propulsion and Power*, Vol. 19, No. 3, May–June 2003, pp. 497–505.

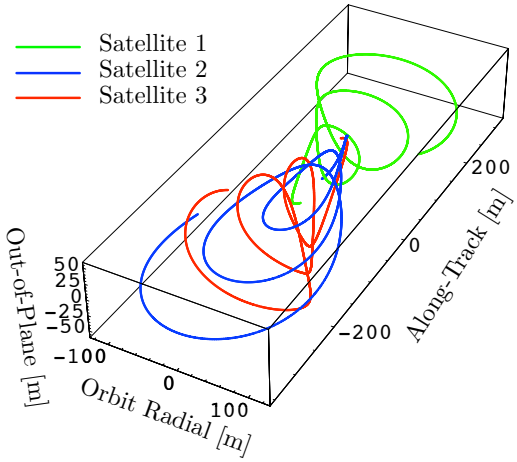

a) No Active Spacecraft Charging

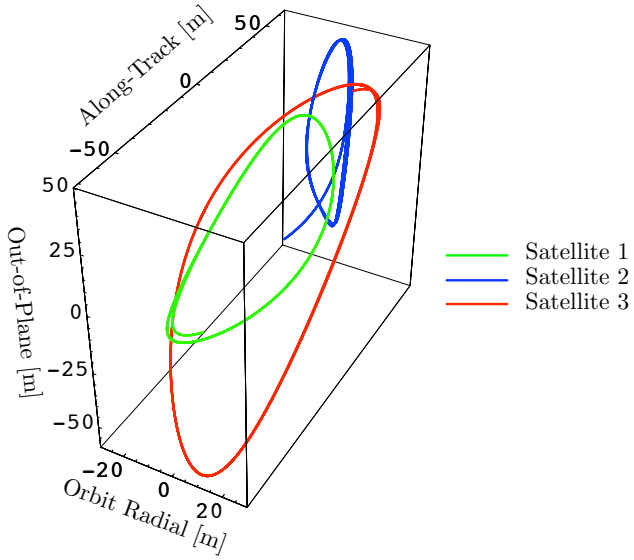

b) With the Spacecraft Charging Control Law Active

Fig. 2 Three-Dimensional Relative Orbit Illustration in the Rotating Chief LVLH Coordinate Frame.

[4]Torkar, K. and et. al., "Active Spacecraft Potential Control for Cluster – Implementation and First Results," *Annales Geophysicae*, Vol. 19, 2001, pp. 1289–1302.

[5]Nicholson, D. R., *Introduction to Plasma Theory*, Krieger, 1992.

[6]Gombosi, T. I., *Physics of the Space Environment*, Cambridge University Press, 1998.

[7]Schaub, H., Parker, G. G., and King, L. B., "Challenges and Prospect of Coulomb Formations," *AAS John L. Junkins Astrodynamics Symposium*, College Station, TX, May 23-24 2003, Paper No. AAS-03-278.

[8]Battin, R. H., *An Introduction to the Mathematics and Methods of Astrodynamics*, AIAA Education Series, New York, 1987.

[9]Schaub, H. and Junkins, J. L., *Analytical Mechanics of Space Systems*, AIAA Education Series, Reston, VA, October 2003.

[10]Ilgen, M. R., "Low Thrust OTV Guidance using Lyapunov Optimal Feedback Control Techniques," AAS/AIAA Astrodynamics Specialist Conference, Victoria, B.C., Canada, Aug. 16–19 1993, Paper No. AAS 93-680.

[11]Naasz, B. J., *Classical Element Feedback Control for Spacecraft Orbital Maneuvers*, Master's thesis, Virginia Polytechnic Institute and State University, Blacksburg, VA, May 2002.

[12]Naasz, B. J., Karlgaard, C. D., and Hall, C. D., "Application of Several Control Techniques for the Ionospheric Observation Nanosatellite Formation," AAS/AIAA Space Flight Mechanics Meeting, San Antonio, TX, Jan. 2002, Paper No. AAS 02-188.

[13]Broucke, R. A. and Cefola, P. J., "On the Equinoctial Orbit Elements," *Celestial Mechanics*, Vol. 5, 1972, pp. 303–310.

[14]Slotine, J. E. and Li, W., *Applied Nonlinear Control*, Prentice-Hall, Inc., Englewood Cliffs, New Jersey, 1991.

[15]Khalil, H. K., *Nonlinear Systems*, Prentice-Hall, Inc., Upper Saddle River, NJ, 3rd ed., 2002.

[16]Schaub, H., "Relative Orbit Geometry Through Classical Orbit Element Differences," *Journal of Guidance, Control and Dynamics*, Vol. 27, No. 5, Sept.–Oct. 2004, pp. 839–848.